Transfer printing by kinetic control of adhesion to an elastomeric stamp

MATTHEW A. MEITL[1,2], ZHENG-TAO ZHU[1,2], VIPAN KUMAR[3], KEON JAE LEE[1,2], XUE FENG[4], YONGGANG Y. HUANG[4], ILESANMI ADESIDA[3], RALPH G. NUZZO[1,2] AND JOHN A. ROGERS[1,2]*

[1]Department of Materials Science and Engineering, Beckman Institute, and Seitz Materials Research Laboratory, University of Illinois at Urbana-Champaign, 1304 West Green Street, Urbana, Illinois 61801, USA

[2]Department of Chemistry, Beckman Institute, and Seitz Materials Research Laboratory, University of Illinois at Urbana-Champaign, 1304 West Green Street, Urbana, Illinois 61801, USA

[3]Department of Electrical and Computer Engineering, Micro and Nanotechnology Laboratory, University of Illinois at Urbana-Champaign, Urbana, Illinois 61801, USA

[4]Department of Mechanical and Industrial Engineering, University of Illinois at Urbana-Champaign, Urbana, Illinois 61801, USA

*e-mail: jrogers@uiuc.edu

Published online: 11 December 2005; doi:10.1038/nmat1532

An increasing number of technologies require large-scale integration of disparate classes of separately fabricated objects into spatially organized, functional systems[1–9]. Here we introduce an approach for heterogeneous integration based on kinetically controlled switching between adhesion and release of solid objects to and from an elastomeric stamp. We describe the physics of soft adhesion that govern this process and demonstrate the method by printing objects with a wide range of sizes and shapes, made of single-crystal silicon and GaN, mica, highly ordered pyrolytic graphite, silica and pollen, onto a variety of substrates without specially designed surface chemistries or separate adhesive layers. Printed p–n junctions and photodiodes fixed directly on highly curved surfaces illustrate some unique device-level capabilities of this approach.

Examples of systems that rely critically on heterogeneous integration range from optoelectronic systems that integrate lasers, lenses and optical fibres with control electronics[1–3], to tools for neurological study that involve cells interfaced to arrays of inorganic sensors[4], to flexible 'macroelectronic' circuits and actuators that combine inorganic device components with thin plastic substrates[5–9]. The most significant challenges associated with realizing these types of system derive from the disparate nature of the materials and the often vastly different techniques needed to process them into devices. As a result, all broadly useful integration strategies begin with independent fabrication of components followed by assembly onto a single device substrate.

This letter introduces a deterministic, high-speed approach for manipulation and heterogeneous integration that uses kinetically controlled adhesion to elastomeric transfer elements, or stamps, to transfer print solid objects from one substrate to another. This technique provides an important combination of capabilities that is not offered by other assembly methods, such as those based on 'pick and place' technologies, wafer bonding[10] or directed self-assembly[2,8,11–14]. Figure 1 schematically illustrates the process, beginning with the preparation of a donor substrate that supports fully formed, organized arrays of solid objects (for example, devices, materials elements, biological entities and so on). The donor substrate can be prepared using top-down fabrication, bottom-up growth, self-assembly or other means. Contacting a soft elastomeric stamp against these solid objects leads to conformal contact, driven by generalized adhesion forces that are typically dominated by van der Waals interactions[15,16]. The adhesion between the solid objects and the stamp is rate-sensitive (that is, kinetically controllable) owing to the viscoelastic behaviour of the elastomer. Pulling the stamp away from the donor substrate with sufficiently high peel velocity (typically $\sim$10 cm s^{-1} or faster for the systems presented here) leads to adhesion that is strong enough to adhere preferentially the solid objects to the surface of the stamp, lifting them away from the substrate. The stamp, now 'inked' with these objects, is brought into contact with a receiving (device) substrate. Removing the stamp with sufficiently low peel velocity ($\sim$1 mm s^{-1} or slower) causes the objects to adhere preferentially to the device substrate and separate from the stamp. The transfer can be carried out uniformly with a flat stamp or with a structured element that contacts and transfers only some set of objects from the donor substrate.

The physics that governs the kinetic dependence of the adhesion process has its origin in the viscoelastic response of the elastomeric stamp. We performed rolling experiments[17,18] to yield quantitative information on this dependence for the case of a commercially available polydimethylsiloxane (PDMS) rubber (Sylgard 184, Dow Corning). In these experiments, a steel cylinder rolling down an inclined slab of PDMS rubber reaches a terminal velocity, where gravity works to separate the steel from the PDMS at the trailing edge of the contact region. The loss in gravitational potential is taken as the adhesion energy hysteresis (the difference between the work required to separate the steel from the PDMS and the energy evolved at the advancing contact edge) at the measured rolling

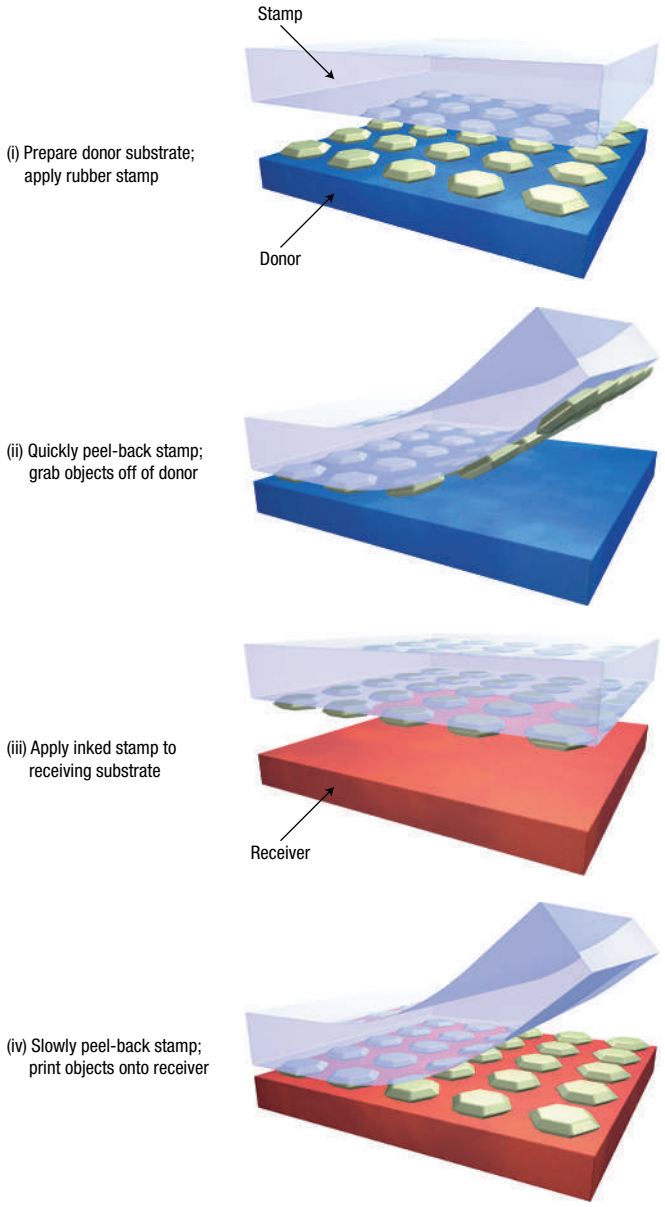

Figure 1 Schematic illustration of the generic process flow for transfer printing solid objects. The process begins with the preparation of an assemblage of microstructures on a donor substrate by solution casting, micromachining, self-assembly or other suitable means. (i) Laminating a stamp against a donor substrate and then quickly peeling it away (ii) pulls the microstructures from the donor substrate onto the stamp. Contacting the stamp to another substrate (receiving substrate (iii)) and then slowly peeling it away transfers the microstructures from the stamp to the receiver (iv). The peeling rate determines the strength of adhesion and, therefore, the direction of transfer.

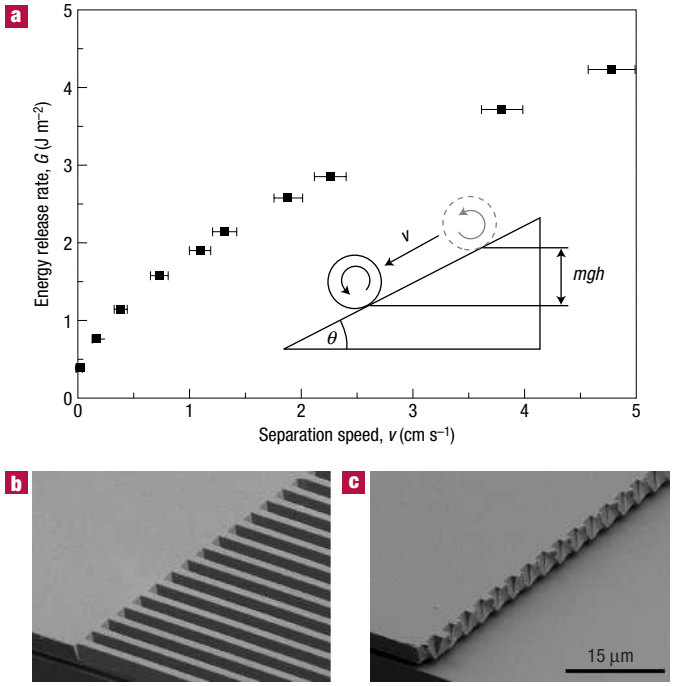

Figure 2 Rate dependence of stamp adhesion. The glueless transfer printing strategy described here relies on the relatively strong adhesion of rubber to solids at fast peel rates, v, and significantly weaker adhesion at slower rates. **a**, The rate-dependent adhesion causes a steel cylinder rolling down an inclined slab of PDMS to assume a constant speed dependent on the angle of inclination θ, allowing calculation of the energy release rate, G, from the loss of gravitational potential energy. The error bars are the standard deviation in the set of rolling speeds measured at each incline. Across the range of speeds measured here, G varies by more than an order of magnitude. **b**,**c**, Slow removal of a PDMS stamp from the micromachined silicon beams in **b** leaves them intact, but the much higher adhesive force associated with fast (~10 cm s^{-1} or faster) stamp removal cleanly breaks the structures from their anchor (**c**).

or separation speed v. The energy associated with the advancing contact area at the front of the rolling cylinder is typically small[19], so the adhesion energy hysteresis is taken as the separation energy, or the energy release rate, G. Figure 2 shows the dependence of G on v. For the range of speeds measured here (0.02 to 4.8 cm s^{-1}), the energy release rate varies by more than an order of magnitude.

Observed pick-up and printing efficiencies in transfer-printing experiments follow a similar trend qualitatively. When a PDMS stamp delaminates slowly from a substrate that supports microstructures, the separation energy G_{PDMS} for the elastomer–microstructure interface is smaller than its counterpart $G_{substrate}$ for the interface between the microstructures and the substrate. Consequently the elastomer–microstructure interface breaks more easily than the microstructure–substrate interface. However, the separation energy G_{PDMS} depends strongly on the speed of delamination v (see, for example, Fig. 2a and refs 20,21) owing to the viscous behaviour of PDMS, that is, $G_{PDMS} = G_0[1 + \phi(v)]$ where ϕ is an increasing function of v. In contrast, the separation energy for the microstructure–substrate interface $G_{substrate}$ is typically independent of rate. As the speed of delamination increases, G_{PDMS} increases relative to $G_{substrate}$ until the elastomer–microstructure interface becomes strong enough to break the microstructure–substrate interface. Exact criteria for determining which interface fails are beyond the scope of this text, but they depend on the geometry of the microstructures and can be established by energy-based arguments similar to those used to compare competing fracture modes in layered materials[22]. The key concept for the transfer-printing criteria is the strongly rate-dependent separation energy of solid objects from an elastomer. As an example of a type of structure the transfer elements can retrieve from a donor, Fig. 2b shows freestanding silicon beams micromachined from a silicon-on-insulator (SOI) wafer, connected to an unetched part of the wafer that anchors

their ends. Application and slow removal of a stamp from these robust, freestanding structures leaves them intact. Fast removal, however, fractures them cleanly at their ends (Fig. 2c) and leaves them adhered to the stamp. The stamp, thus 'inked' with the silicon beams, can transfer those beams by contact to and slow removal from a receiving substrate.

Figure 3a shows a 30 mm × 38 mm array of such wafer-generated objects (I-shaped silicon microstructures) printed in ambient conditions directly onto a 100-mm GaAs wafer. This array contains about 24,000 microstructures; the yield of the entire process, including micromachining, pick-up and printing, is more than 99.5%. Particles on the surface of the receiving substrate are typically the most significant cause of defects. Unlike wafer-bonding approaches to semiconductor materials integration, printing also has the potential for area multiplication[23], where a single donor substrate of a given area supplies microstructures to several receiving substrates of the same area or a single receiving substrate with a substantially larger area. This capability is important when the printed material is costly and where large-area, sparse coverage is desired. GaN microstructures prepared as described in the methods section and printed onto silicon (100), as shown in Fig. 3b, is an example of one of these systems. As the transfer process is purely additive, repeated printing is straightforward, allowing easy fabrication of large-area or even multilayer assemblies (Fig. 3c) with few processing steps for applications as photonic bandgap materials[24,25] or multilayer electronic systems.

The technique can print objects with a wide range of shapes and sizes onto virtually any smooth substrate. Submicrometre (0.3 μm × 20 μm × 0.1 μm) silicon structures printed onto InP in Fig. 3d suggest that stamp-based transfer printing can apply to device-scale or smaller objects. At larger sizes (100 μm × 100 μm × 2.5 μm), printing can apply to structures that might support elaborate circuits (Fig. 3e). Yields for printing large objects are generally lower than for small objects, as a single asperity between a printed object and receiving substrate can impede transfer. Nevertheless, yields of 95% or better are easily achievable for all of the wafer-generated geometries presented here when the receiving substrate is smooth, even when the printing is performed outside a cleanroom environment. Substrates with surface roughness of less than ~3 nm over 1 μm^2 can function as effective receivers, largely independent of chemical composition or surface energy. For example, silicon microstructures can reliably transfer onto either hydrophilic surfaces, such as SiO_2, NaCl and MgO (Fig. 3f), or hydrophobic surfaces, from polystyrene to silicon freshly stripped of its native oxide.

The absence of conventional adhesives or specialized surface chemistries is valuable in the context of wafer-based microstructure printing because it allows moderate-to-high-temperature processing and good electrical contact between the printed structure and the receiving substrate. Printed p–n junctions formed by transferring n-type silicon microstructures to a p-type silicon substrate (Fig. 3g) exploit both of these features. Annealing and metallization of the junction produces a rectifying device with characteristics reasonably well described by a fit for a monolithic p–n junction as the applied bias sweeps from −1 to 1 V. The fit in Fig. 3g is characteristic of a diode with an ideality factor of 1.7 and a reverse saturation current of 0.9 nA shunted with a 2 GΩ resistor and in series with a 400 Ω resistor. At 1 V bias, this printed junction supports a current of about 6.7 A cm^{-2}.

The remarkably strong adhesion to the stamp at high peel rates is essential to achieve reliable, high-yield printing of the classes of objects illustrated in Figs 2 and 3. This adhesion can be sufficiently strong, in fact, to remove material structures that are ionically bonded to the donor substrate along their entire lengths. Figure 4a shows, as an example, patterns of thin high-quality muscovite (grade V-1 mica) printed by removing a stamp in contact with

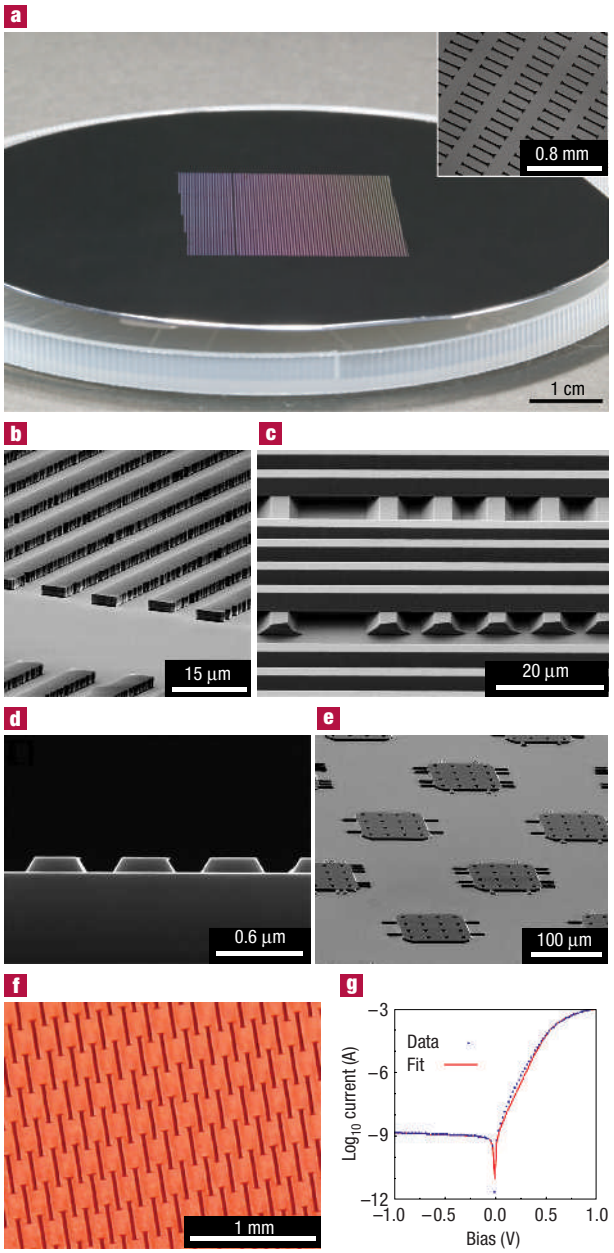

Figure 3 Images of transfer-printed objects derived from semiconductor wafers that demonstrate a range of capabilities. a, 30 mm × 38 mm array of about 24,000 silicon microstructures printed onto a 100-mm GaAs wafer. Inset scanning electron microscope image (Philips XL30 ESEM-FEG, FEI). Fewer than 100 microstructures are missing from the array. **b**, GaN ribbons printed onto a silicon (100) wafer. **c**, Multilayer stack of crossed silicon ribbons formed by printing onto a silicon wafer. **d**,**e**, Printed silicon structures with a wide range of shapes and sizes, from submicrometre-scale objects that would be difficult to manipulate using other means, to objects sufficiently large to support fully integrated electronic or mechanical devices. **d**, p-type silicon printed onto InP. **e**, n-type silicon printed onto p-type silicon. **f**, Silicon structures printed onto a translucent MgO substrate (hydrophilic). **g**, n-type silicon structures printed onto a p-type silicon wafer (hydrophobic) to form p–n junctions that can carry 6.7 A cm^{-2} at a forward bias of 1 V. The red line is a fit to the data points.

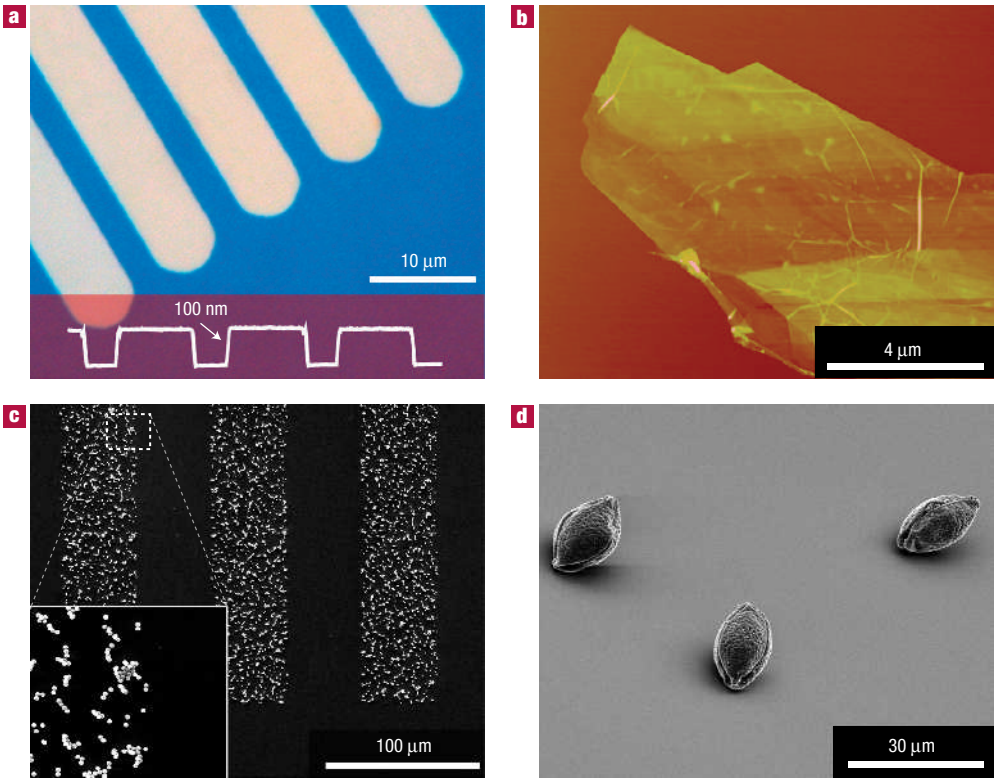

Figure 4 Images of transfer printed objects with sheet-like and globular geometries. a, 100-nm-thick mica ribbons cleaved from a mica substrate with a PDMS stamp, and then transfer-printed onto SiO_2 (blue). **b**, Graphite sheet, ranging from 3 to 12 nm thick, cleaved from a highly ordered pyrolytic graphite substrate and printed onto SiO_2 with a stamp. **c**,**d**, Silica microspheres (**c**) and African Violet pollen grains (**d**) picked up from and subsequently printed onto silicon wafers by means of PDMS stamps. Relief features in the stamp define the stripe pattern in **c**.

the mica at sufficiently high peel rates to cleave patterned ribbons from a donor substrate of bulk mica. PDMS stamps can also cleave sheets from unpatterned grade V-1 mica or graphite (Fig. 4b) and lift off mica sheets bonded to SiO_2, indicating that the stamp–microstructure interface is strong enough at high peel rates to remove structures bound to a donor substrate at least as strongly as 6 J m^{-2} (ref. 26). The high adhesive strength present at high peel rates reduces to minimal levels at low rates. Stamps can even release, for example, highly non-planar, globular structures, such as silica microspheres and grains of pollen (Fig. 4c,d), which have very small areas of contact to rigid receiving substrates.

Transfer printing in this manner has many potential applications in established technologies: its unusual capabilities may create other device opportunities. To illustrate one such capability, we printed silicon structures and photodiodes onto the curved surfaces of lenses. Non-planar printing proceeds by rolling a cylindrical substrate across or by pressing a spherical substrate against a flat, compliant stamp. Figure 5 shows arrays of silicon microstructures printed onto a cylindrical glass lens and onto a low-cost spherical polycarbonate lens. This figure also illustrates fully functional single-crystal silicon photodiodes printed onto a glass lens with the current–voltage characteristics of a typical device. We believe that such non-planar microfabrication will be valuable for applications including light detection and energy generation on curved focusing or imaging optics.

The method presented here represents a powerful way to manipulate arrays of objects based on kinetically controllable adhesion to a viscoelastic stamp in a massively parallel and deterministic manner. The mechanics suggest paths for optimizing the material properties of the stamps in ways that have not been explored in soft lithography or related areas. Even with existing materials, the printing procedure provides robust capabilities for generating microstructured hybrid materials systems and device arrays with potential applications in optoelectronics, photonics, non-planar fabrication and perhaps even biotechnology without the use of glues, moving parts, applied electric or magnetic fields. In these ways, stamp-based methods may become invaluable tools for handling the building blocks of nano- and other emerging technologies.

METHODS

ROLL TEST

A slab of PDMS (Dow-Sylgard 184) was cast between two 200 mm silicon wafers separated by ~7 mm using PDMS spacers and cured at 65 °C. The wafers were treated with (tridecafluoro-1,1,2,2-tetrahydrooctyl)-1-trichlorosilane (United Chemical Technologies) for 1 h in a vacuum desiccator to facilitate the removal of the PDMS slab. The slab was placed against a sturdy inclined glass plate, the inclination of which was measured relative to a level countertop. A steel cylinder (McMaster-Carr, diameter 12.7 mm, length 75.5 mm, 75.2 g) was placed at the top of the slab and allowed to roll. The slab was cleaned with a lint roller (3M) between successive roll tests. Rolling speed was measured with a ruler and a stopwatch. Video footage was captured and analysed to confirm that the cylinder rolled against the slab at a constant speed.

DONOR SUBSTRATE PREPARATION

Silicon microstructures were generated from SOI wafers (Shin-Etsu, top silicon 3.0 μm, buried oxide 1.1 μm, n-type resistivity 5–20 Ω cm; or Soitec, top silicon 100 nm, buried oxide 200 nm, p-type) patterned by conventional

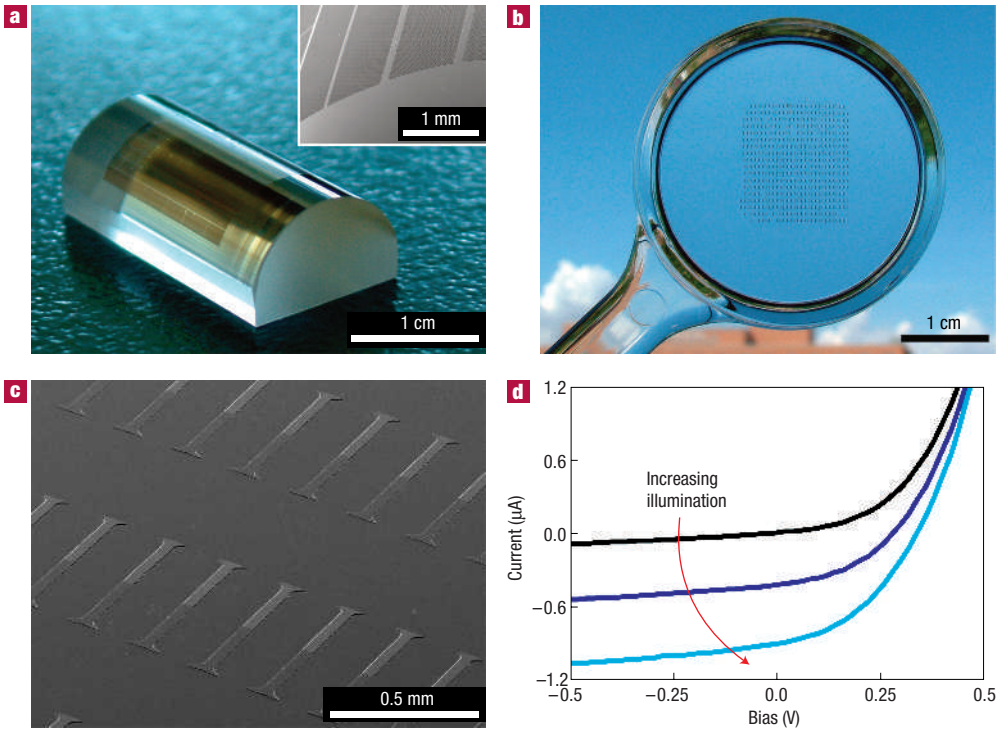

Figure 5 Silicon microstructures and solar cells printed onto curved surfaces by rolling and pressing. a, Printed array formed by rolling a cylindrical glass lens across a stamp inked with microstructures with inset scanning electron microscope image. **b**, Printed array formed by pressing a double-convex polycarbonate magnifying glass into the soft, inked stamp. **c**, Silicon photodiodes printed on a spherical glass surface (p-doped regions seem brighter). **d**, Current–voltage characteristics of a typical printed device under different illumination conditions.

photolithography and phase-shift photolithography[27] with Shipley 1805 photoresist (PR). The top silicon was etched by SF_6 plasma (30 mtorr, 40 s.c.c.m. SF_6, 50 W) using PR as an etch mask or by aqueous KOH (20 wt%, 100 °C) using an etch mask of Ti/Au (3/30 nm) deposited by electron-beam evaporation. Ti/Au etch masks were removed after KOH etching using KI/I_2 (2.67/0.67 wt%) in water. The buried oxide was then etched in concentrated HF.

GaN microstructures were generated from a GaN-on-silicon (111) wafer (Nitronex). The nitride was etched in an inductively coupled plasma reactive ion etcher (3 mtorr, 15 s.c.c.m. Cl_2, 5 s.c.c.m. Ar, −100 V bias) using PECVD SiO_x (500 nm) and Cr (150 nm) as an etch mask. Microstructures were then undercut by etching the silicon in aqueous KOH (20 wt%, 100 °C).

Mica (grade V-1, Structure Probe) was softened in an inductively coupled plasma reactive ion etcher (3 mtorr, 15 s.c.c.m. BCl_3, 5 s.c.c.m. Ar, −90 V bias) using electron-beam evaporated Cr (100 nm) and PR as a mask. Unpatterned grade V-1 mica and graphite substrates (grade SPI-1, Structure Probe) were used as-received.

Silica microsphere films were prepared by casting droplets of IPA and an aqueous suspension of microspheres onto a silicon wafer and allowing them to dry. Pollen films were also prepared by suspension casting and drying on a silicon wafer.

TRANSFER

PDMS stamps (Dow-Sylgard 184) were cast against flat substrates (for example, polystyrene petri dishes, Fisher Scientific) and cut to dimensions typically ~2 cm × 2 cm × 7 mm thick. Stamps were laminated against donor substrates such that conformal contact was achieved and subsequently removed manually in a peeling manner such that the delamination front travelled at 10 cm s^{-1} or faster. The stamps thus 'inked' with objects from the donor were then laminated against receiving substrates and subsequently removed by slow (~1 mm s^{-1}) manual peeling to complete the transfer-printing process.

PRINTED JUNCTION DIODE FABRICATION

SOI chips (Shin-Etsu) were heavily n-doped at the top surface with spin-on-dopant[6] (P509, Filmtronics) and activation at 950 °C for 5 s. Microstructures generated as described above were printed onto boron-doped test-grade silicon chips (Montco, resistivity 1–100 Ω cm). Before printing, the receiving substrate was dipped in ~1% HF to remove native oxide, rinsed with deionized water and dried in N_2. The printed junction was then annealed for 2 min at 600 °C in N_2. Metal contacts were defined by photolithography with Shipley 1818 and lift-off of electron-beam-evaporated Al/Au (20/50 nm). The contacts were made non-rectifying by 4 min of annealing at 500 °C.

PHOTODIODE FABRICATION

Silicon photodiodes were generated from an n-type SOI wafer (Shin-Etsu) with selected areas highly n-doped (P509, Filmtronics) and other areas highly p-doped (B-75X, Honeywell). Doped regions were defined using windows in a spin-on glass (700B, Filmtronics) and the dopants were activated by annealing as described above[6] for the printed junction fabrication, first n-type, then p-type. Structures were subsequently micromachined using SF_6 plasma and undercut with HF.

Received 28 July 2005; accepted 26 September 2005; published 11 December 2005.

References

1. Georgakilas, A. *et al.* Wafer-scale integration of GaAs optoelectronic devices with standard Si integrated circuits using a low-temperature bonding procedure. *Appl. Phys. Lett.* **81,** 5099–5101 (2002).
2. Yeh, H.-J. J. & Smith, J. S. Fluidic self-assembly for the integration of GaAs light-emitting diodes on Si substrates. *IEEE Photon. Technol. Lett.* **6,** 706–708 (1994).
3. Ambrosy, A., Richter, H., Hehmann, J. & Ferling, D. Silicon motherboards for multichannel optical modules. *IEEE Trans. Compon. Pack. A* **19,** 34–40 (1996).
4. Lambacher, A. *et al.* Electrical imaging of neuronal activity by multi-transistor-array (MTA) recording at 7.8 μm resolution. *Appl. Phys. A* **79,** 1607–1611 (2004).
5. Menard, E., Lee, K. J., Khang, D.-Y., Nuzzo, R. G. & Rogers, J. A. A printable form of silicon for high performance thin film transistors on plastic substrates. *Appl. Phys. Lett.* **84,** 5398–5400 (2004).
6. Zhu, Z.-T., Menard, E., Hurley, K., Nuzzo, R. G. & Rogers, J. A. Spin on dopants for high-performance single-crystal silicon transistors on flexible plastic substrates. *Appl. Phys. Lett.* **86,** 133507 (2005).
7. Sun, Y. & Rogers, J. A. Fabricating semiconductor nano/microwires and transfer printing ordered arrays of them onto plastic substrates. *Nano Lett.* **4,** 1953–1959 (2004).
8. Jacobs, H. O., Tao, A. R., Schwartz, A., Gracias, D. H. & Whitesides, G. M. Fabrication of a cylindrical display by patterned assembly. *Science* **296,** 323–325 (2002).
9. Reuss, R. H. *et al.* Macroelectronics: Perspectives on technology and applications. *Proc. IEEE* **93,** 1239–1256 (2005).
10. Haisma, J. & Spierings, G. A. C. M. Contact bonding, including direct-bonding in a historical and recent context of materials science and technology, physics and chemistry—historical review in a broader scope and comparative outlook. *Mater. Sci. Eng. R* **37,** 1–60 (2002).

11. Zheng, W. & Jacobs, H. O. Shape-and solder-directed self-assembly to package semiconductor device segments. *Appl. Phys. Lett.* **85,** 3635–3637 (2004).
12. Bowden, N., Terfort, A., Carbeck, J. & Whitesides, G. M. Self-assembly of mesoscale objects into ordered two-dimensional arrays. *Science* **276,** 233–235 (1997).
13. O'Riordan, A., Delaney, P. & Redmond, G. Field configured assembly: programmed manipulation and self-assembly at the mesoscale. *Nano Lett.* **4,** 761–765 (2004).
14. Tanase, M. *et al.* Magnetic trapping and self-assembly of multicomponent nanowires. *J. Appl. Phys.* **91,** 8549–8551 (2002).
15. Hsia, K. J. *et al.* Collapse of stamps for soft lithography due to interfacial adhesion. *Appl. Phys. Lett.* **86,** 154106 (2005).
16. Huang, Y. Y. *et al.* Stamp collapse in soft lithography. *Langmuir* **21,** 8058–8068 (2005).
17. Roberts, A. D. Looking at rubber adhesion. *Rubber Chem. Technol.* **52,** 23–42 (1979).
18. Barquins, M. Adherence, friction and wear of rubber-like materials. *Wear* **158,** 87–117 (1992).
19. Shull, K. R., Ahn, D., Chen, W.-L., Flanigan, C. M. & Crosby, A. J. Axisymmetric adhesion tests of soft materials. *Macromol. Chem. Phys.* **199,** 489–511 (1998).
20. Brown, H. R. The adhesion between polymers. *Annu. Rev. Mater. Sci.* **21,** 463–489 (1991).
21. Deruelle, M., Léger, L. & Tirrell, M. Adhesion at the solid-elastomer interface: influence of interfacial chains. *Macromolecules* **28,** 7419–7428 (1995).
22. Hutchinson, J. W. & Suo, Z. Mixed mode cracking in layered materials. *Adv. Appl. Mech.* **29,** 63–191 (1992).
23. Lee, K. J. *et al.* Large-area, selective transfer of microstructured silicon (μs-Si): a printing-based approach to high-performance thin-film transistors supported on flexible substrates. *Adv. Mater.* **17,** 2332–2336 (2005).
24. Aoki, K. *et al.* Microassembly of semiconductor three dimensional photonic crystals. *Nature Mater.* **2,** 117–121 (2003).
25. Noda, S., Yamamoto, N. & Sasaki, A. New realization method for three-dimensional photonic crystal in optical wavelength region. *Jpn J. Appl. Phys.* **35,** L909–L912 (1996).
26. Horn, R. G. & Smith, D. T. Contact electrification and adhesion between dissimilar materials. *Science* **256,** 362–364 (1992).
27. Rogers, J. A., Paul, K. E., Jackman, R. J. & Whitesides, G. M. Using an elastomeric phase mask for sub-100 nm photolithography in the optical near field. *Appl. Phys. Lett.* **70,** 2658–2660 (1997).

Acknowledgements

The authors thank A. Shim for helpful discussions, A. Jerez for help generating schematic cartoons, J. Rinne for supplying silica microspheres, J. Lyding for the use of his AFM, and C. J. Hubert for the use of her African Violets. This work was supported by DARPA-funded AFRL-managed Macroelectronics Program Contract FA8650-04-C-7101, the US Department of Energy under grant DEFG02-91-ER45439, the National Science Foundation under grant DMII-0328162, and a graduate fellowship from the Fannie and John Hertz Foundation.
Correspondence and requests for materials should be addressed to J.A.R.

Competing financial interests

The authors declare that they have no competing financial interests.